Weather and Climate Extremes 38 (2022) 100526

Contents lists available at ScienceDirect

Weather and Climate Extremes

journal homepage: www.elsevier.com/locate/wace

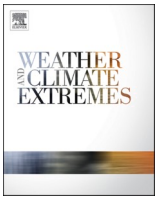

Introducing NARCliM1.5: Evaluation and projection of climate extremes for southeast Australia

Fei Ji [a,c,*], Nidhi Nishant [b,c], Jason P. Evans [b,c], Giovanni Di Virgilio [a,b,c], Kevin K.W. Cheung [d], Eugene Tam [a], Kathleen Beyer [a,e], Matthew L. Riley [a]

[a] Science, Economics and Insights Division, NSW Department of Planning and Environment, Sydney, Australia
[b] Climate Change Research Centre, University of New South Wales, Sydney, Australia
[c] Australian Research Council Centre of Excellence for Climate Extremes, University of New South Wales, Sydney, Australia
[d] E3-Complexity Consulting, Sydney, Australia
[e] School of Geography, Planning and Spatial Sciences, University of Tasmania, Hobart, Australia

ARTICLE INFO

Keywords:
Climate extreme
ET-SCI
NARCliM
Evaluation
Future projections

ABSTRACT

NARCliM1.5 is the second generation of New South Wales and Australian Regional Climate Modelling (NARCliM) project, which is designed to produce an ensemble of regional climate projections for CORDEX Australasia and southeast Australia. The selected global climate models (GCMs) are used to drive Weather Research and Forecasting (WRF) model for dynamical downscaling. In this study, we evaluate how well the two generations of NARCliM (N1.0 and N1.5) represent the observed record for 12 selected climate extremes and examine their projected changes for southeast Australia. N1.5 ensemble substantially improves upon N1.0 in capturing the spatial patterns of precipitation extremes, however, there is little difference between the two ensembles for temperature extremes. Both N1.0 and N1.5 underestimate dry extreme (consecutive dry day - CDD), hot extremes (warmest daily maximum temperature – TXx, and number of days when maximum temperature is greater than 35 °C - TXge35) and daily temperature range (DTR) but overestimate wet extremes (annual sum of daily precipitation above 99th percentile - R99p, consecutive wet days - CWD, days when precipitation is at least 10 mm - R10mm, maximum 1-day precipitation - Rx1Day and total wet day precipitation -PRCPTOT) and cold extreme (coldest daily minimum temperature - TNn). N1.0 and N1.5 project different spatial patterns of future changes in precipitation extremes but similar changes in temperature extremes. Differences in climate extremes between N1.0 and N1.5 could be attributed to the driving GCMs. The combined future projections of both N1.0 and N1.5 provide a more complete sampling of the future change space. Future projections indicate that precipitation and temperature extremes will become more intense, raising implications for future planning and risk management.

1. Introduction

Extreme climate events have damaging impacts on human societies, ecosystems, and economies, both globally and in Australia (Seneviratne et al., 2012). Multiple studies indicate that climate change has increased frequency and/or intensity of extreme temperature and precipitation events (Fischer and Knutti, 2015; Perkins-Kirkpatrick and Gibson, 2017; Prein et al., 2017; Wang et al., 2017). Globally, about 18% of moderate daily precipitation extremes over land and about 75% moderate daily hot extremes over land are attributable to observed warming (Fischer and Knutti, 2015). Climate extremes can result in 18%–43% (the range describes the differences between crop types) of variance of global crop yield anomalies (Vogel et al., 2019). Heat related extremes in Australia lead to annual economic burden of around $6.2 billion for the Australian workforce (Zander et al., 2015).

Global climate models (GCMs) have been used as a primary tool for examining the past and future changes in climate extremes at global and continental scales (Alexander and Arblaster 2017; Ongoma et al., 2018; Ayugi et al., 2021). However, their coarse resolutions mean they are not suitable for regional and local applications (Ekström et al., 2015). Dynamical downscaling of coarse resolution outputs from GCMs via regional climate models (RCMs) helps better resolve the drivers of regional climate, e.g., complex topography, convective processes, and produce climate projections at high resolution. RCM simulations are

* Corresponding author. Science, Economics and Insights Division, NSW Department of Planning and Environment, Sydney, Australia.
E-mail address: fei.ji@environment.nsw.gov.au (F. Ji).

https://doi.org/10.1016/j.wace.2022.100526
Received 17 July 2022; Received in revised form 30 September 2022; Accepted 3 November 2022
Available online 12 November 2022

fundamental components for climate services on national (e.g., Kjellström et al., 2016; Skelton et al., 2017) and regional scales (e.g., Jacob et al., 2014). Multiple studies have reported that downscaling can improve accuracy of the historical simulated climate when comparing to the driving GCMs (Di Luca et al., 2013, 2016a; Torma et al., 2015; Dosio et al., 2015, 2019; Cheneka et al., 2016; Choudhary et al., 2019; Lee et al., 2019; Solman and Blázquez 2019; Gnitou et al., 2021; Qiu and Im, 2021).

Multiple studies have used regional climate simulations to assess future changes in climate extremes such as extreme rainfall (Bao et al., 2017; Evans et al., 2017), climate extreme indices (Herold et al., 2021) and extreme fire weather (Di Virgilio et al., 2019), which highlighted the importance of regional climate modelling in assessment of future changes in climate extremes at regional scales.

The NARCliM (**N**ew South Wales and **A**ustralian **R**egional **Cli**mate **M**odelling) project is designed to produce 50 km and 10 km resolutions regional climate projections for Australasia and Southeast Australia, respectively (Fig. 1) (Evans et al., 2014). The first generation of NARCliM (N1.0) was delivered in 2014 with several studies having evaluated the N1.0 historical simulations (e.g., Ji et al., 2016; Fita et al., 2016; Olson et al., 2016) and observing that N1.0 can simulate observed climate well, even if most of simulations have wet and cold biases. Other work has demonstrated that N1.0 can provide added value to the simulated surface variables such as precipitation, maximum and minimum temperatures when compared to the driving GCMs (Di Luca et al., 2013, 2016a). Since N1.0 was delivered in 2014, it has been widely applied in long-term planning and scientific research, such as assessing changes in rainfall extremes (Cortés-Hernández et al., 2015; Bao et al., 2017; Nishant and Sherwood, 2021), determining changes in frequency and intensity of extra-tropical low pressure systems (Ji et al., 2015; Pepler et al., 2016; Di Luca et al., 2016b), fire-weather and fuel load projections (Clarke et al., 2016; Clarke and Evans 2019; Di Virgilio et al., 2019), near surface winds (Evans et al., 2018), vertical temperature and temperature inversions (Ji et al., 2018, 2020), quantifying the impact of urban expansion on local temperature extremes (Argüeso et al., 2014, 2015), assessing future changes in cropping (Macadam et al., 2016; Liu et al., 2019; Wang et al., 2019), hydrological impact and wet/dry spells (Evans et al., 2017), and natural hazards (Herold et al., 2021).

Whilst the N1.0 datasets have been applied successfully in multiple contexts, an independent evaluation and multiple technical workshops conducted for end-users have revealed some limitations (Table S1) in the N1.0 experimental design such as older phases of CMIP GCMs (i.e. CMIP3), non-continuous simulations for three discrete 20-years epochs, and use of a single emission scenario. To address those limitations of N1.0, a second generation of enhanced and updated NARCliM simulations (N1.5) was performed.

N1.5 simulations were designed not to replace N1.0 simulations, but rather to complement them. N1.5 simulations are performed using two of the three RCMs used in N1.0 and were run on the same domains as N1.0 to provide an expanded dataset. By using the same RCMs and domains as for N1.0, users can conveniently use either or both the N1.0 and N1.5 datasets without consideration of the impacts from change in the boundary and/or regional model physics. In N1.5, three CMIP5 GCMs were selected and downscaled by two RCMs each for two Representative Concentration Pathways (RCP8.5 and RCP4.5) for 1950–2100, providing 12 regional climate simulations (Nishant et al., 2021).

N1.5 was evaluated and compared with N1.0 for simulating historical mean temperature and precipitation over southeast Australia (Nishant et al., 2021; Di Virgilio et al., 2020). The results indicated that N1.5 simulations substantially improve the skill in capturing seasonal pattens and magnitudes of precipitation, but simulate similar results for maximum and minimum temperatures, when compared with N1.0. Together, N1.0 and N1.5 ensembles provide an improved, more comprehensive data set for studying climate change.

However, it is not clear whether N1.5 simulations can improve skill in capturing climate extremes. In this study we expand the work of Nishant et al. (2021) and assess N1.0 and N1.5 simulations for their

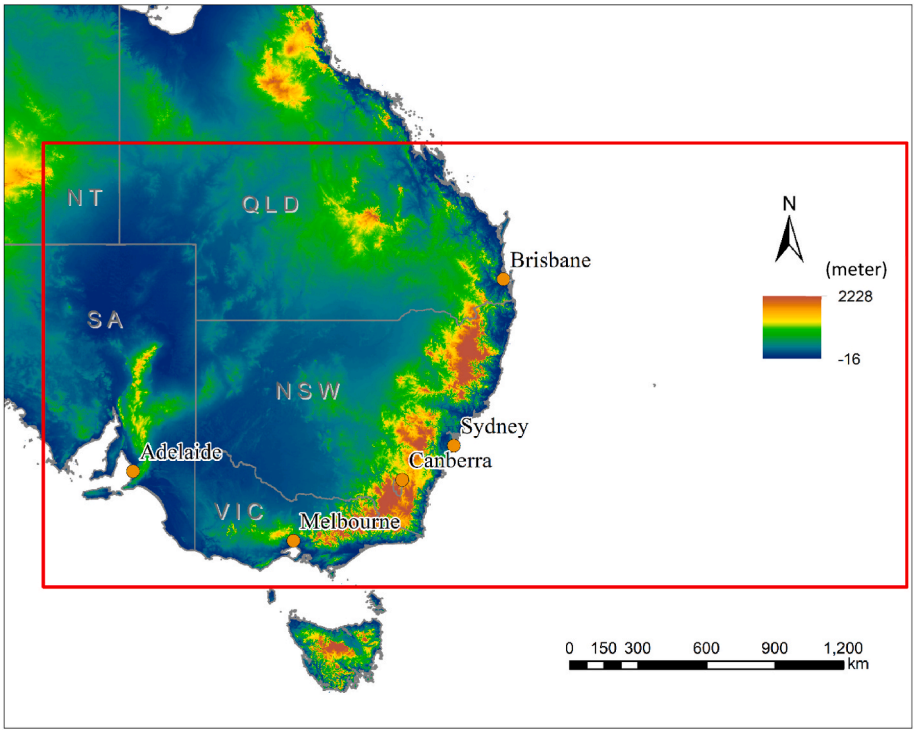

Fig. 1. Map showing Weather Research and Forecasting (WRF) model domain with grid spacing of 10 km (NARCliM domain shown with red outline). QLD, NSW, VIC, SA and NT are initial of Queensland, New South Wales, Victoria, South Australia and Northern Territory, which are Australia's states. Brisbane, Sydney, Melbourne, Adelaide and Canberra are capital cities. (For interpretation of the references to colour in this figure legend, the reader is referred to the Web version of this article.)

ability to simulate observed climate extremes. We undertake and compare future projections of climate extremes for N1.0 and N1.5.

2. Data and methods

2.1. NARCliM1.0 (N1.0)

N1.0 is an ensemble of 12 GCM/RCM combinations (Evans et al., 2014). The four GCMs (MIROC3.2, ECHAM5, CGCM3.1 and CSIRO-MK3.0) were selected from the CMIP3 ensemble based on their model performance over Australasia, independence of their errors, and to span the full range of potential future changes in precipitation and temperature over south-eastern Australia (Fig. 1). Each of these four GCMs were dynamically downscaled using three selected RCMs (R1, R2 and R3). The three RCM configurations are distinct combinations of physics schemes (Table S2) of the Weather Research and Forecasting (WRF) v3.3 model (Skamarock and Klemp, 2008), which were selected from 36 physics scheme combinations based on model performance and independence of their errors (Evans et al., 2012, 2013; Evans and Ji 2012; Ji et al., 2014). All RCM simulations were run for three 20-year periods: the recent past (1990–2009), near future (2020–2039) and far future (2060–2079), at 10-km resolution over Southeast Australia, embedded within the 50-km resolution domain of the CORDEX Australasia region (Fig. 1), under the SRES A2 scenario (Solomon et al., 2007) which reflects the 'business-as-usual' scenario in CMIP3 and, at the time of development, best illustrated the assumptions about how global emissions were tracking.

The three selected RCMs were also run by using the National Centres for Environmental Prediction reanalysis dataset (Kalnay et al., 1996) for 1950–2009 to assess the capability of RCMs to simulate the observed regional climate (Ji et al., 2016).

2.2. NARCliM1.5 (N1.5)

N1.5 was designed to address three major limitations in N1.0: the use of older CMIP3 GCMs; a single emission scenario; and the simulation of only a selection of limited time periods. N1.5 consists of three CMIP5 GCMs (ACCESS1.0, ACCESS1.3 and CanESM2) downscaled using two of the three RCMs used in N1.0 for 1951–2100 under two future emission scenarios. The third RCM (R3) from N1.0 was excluded due to unsatisfactory performance (Di Virgilio et al., 2019a). CMIP5 uses emissions scenarios called 'representative concentration pathways' (RCPs) and N1.5 uses both RCP4.5 and RCP8.5. These scenarios reflect a medium level of mitigation and a high emissions scenario, respectively.

The three CMIP5 GCMs were selected using a similar performance evaluation as the CMIP3 GCMs in N1.0. That is, considerations include their performance in simulating temperature and precipitation, representation of various climate processes and phenomena and an independence ranking. In this study we use the highest emission scenario for both generation of GCMs (i.e., SRESA2 from CMIP3 and RCP8.5 from CMIP5). The SRES A2 and RCP8.5 emission scenarios are most comparable yet slightly different. Studies have shown that global climate projections are approximately similar across CMIP3 and CMIP5, especially for temperature increases (Flato and Coauthors, 2013; Knutti and Sedláček 2013; Moise et al., 2015). This suggests that they can be combined into expanded ensembles. We therefore select three CMIP5 GCMs to fill unsampled space within the combined CMIP3 and CMIP5 ensembles. The three selected CMIP5 GCMs have similar temperature increases but spanning the range of precipitation changes from "not much change" to "moderate decrease" to "large decrease" (Nishant et al., 2021). Thus, GCMs in N1.5 complement those in N1.0 in terms of the range of projected climate change (Fig. 2).

Each N1.5 simulation was run from 1950 to 2100 continuously using the WRF model (1950 is taken as spin-up period). We use a newer version of WRF (version 3.6.0) in N1.5 compared to N1.0 (version 3.3) but keep using the same RCM physics configuration. This change, however, did not impact model simulation (Nishant et al., 2021). The 150-year GCM driven simulations are also accompanied by ERA-Interim reanalysis (Dee et al., 2011) forced simulations for 1979–2013. The N1.5 experimental setup is summarised in Table 1 with further information provided in Table S2.

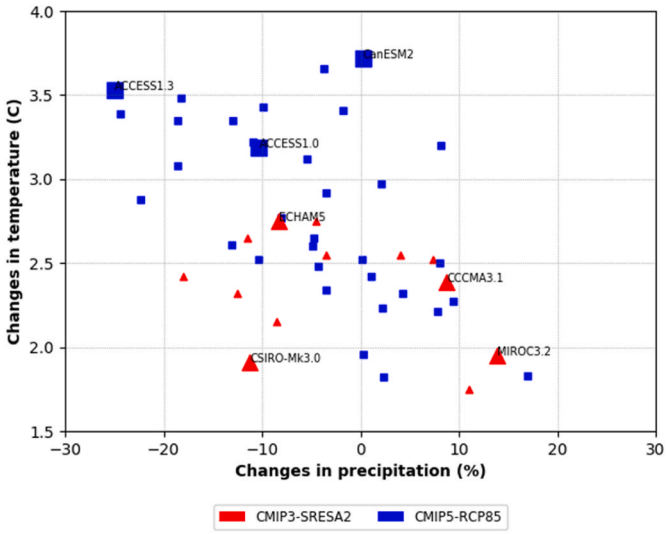

Fig. 2. Scatter plot of future change (differences between 2060-2079 and 1990–2009) in rainfall and temperature over the land part of the NARCliM domain (Fig. 1) for 34 CMIP5 (blue) and 14 CMIP3 (red) GCMs that passed the performance test. Larger dots represent the three GCMs selected for N1.5 (blue) and the four GCMs selected for N1.0 (red). (For interpretation of the references to colour in this figure legend, the reader is referred to the Web version of this article.)

2.3. Observations

The observational data in the study are from the Australian Gridded Climate Dataset (AGCD, Evans et al., 2020). The daily gridded maximum and minimum temperatures, and precipitation data set has a spatial resolution of 0.05° (~5 km) and is interpolated from observations at stations across the Australian continent. Most of those stations are in the more heavily populated coastal regions with far fewer stations inland and over high elevation areas. Observations and simulations are not at the same resolutions. Therefore, for comparison with observations, we interpolate observations to NARCliM grids using the conservative area weighted re-gridding scheme from the Climate Data Operators (Schulzweida et al., 2006).

2.4. Method

While extreme climate and weather events are generally multifaceted phenomena, in this study we evaluate climate extremes based on daily precipitation and temperature as defined by Expert Team on Sector-specific Climate Indices (ET-SCI; Alexander and Herold, 2015; Herold and Alexander, 2016). We use the ClimPACT version 2 software to calculate the ET-SCI indices (https://climpact-sci.org/), focussing on daily precipitation, maximum and minimum temperatures.

Although ClimPACT produces more than 33 core indices, we select 12 indices (Table 2) based on the following considerations: 1). To capture key aspects of climate extremes; for example we choose absolute indices (e.g., maximum 1 day precipitation (Rx1day), total precipitation (PRCPTOT), hottest day (TXx), coldest day (TNn)), threshold-based indices (e.g., number of heavy rain days (R10mm), number of days when maximum temperature is greater than 35 °C (TXge35)), percentile indices (e.g., total annual precipitation from very heavy rain days (R99p)), and duration indices (e.g., consecutive wet days (CWD),

Table 1
NARCliM1.0 and NARCliM1.5 simulations used in this study. Here for clarity, blue and orange colours differentiate between N1.0 and N1.5 simulations.

Simulation-Name	Driving GCM	RCM	WRF Version	Historical period	Future periods	CMIP future pathway
CGCM3.1-R1	CGCM3.1	R1	WRF3.3	1990-2009	2020-2039; 2060-2079	SRES A2
CGCM3.1-R2		R2				
CGCM3.1-R3		R3				
MK3.0-R1	Mk3.0	R1				
MK3.0-R2		R2				
MK3.0-R3		R3				
ECHAM5-R1	ECHAM5	R1				
ECHAM5-R2		R2				
ECHAM5-R3		R3				
MIROC-R1	MIROC	R1				
MIROC-R2		R2				
MIROC-R3		R3				
CanESM2-R1	CanESM2	R1	WRF3.6	1951-2005	2006-2100	RCP8.5
CanESM2-R2		R2				
ACCESS1-0-R1	ACCESS1-0	R1				
ACCESS1-0-R2		R2				
ACCESS1-3-R1	ACCESS1-3	R1				
ACCESS1-3-R2		R2				

consecutive dry days (CDD), warm spell duration index (WSDI), cold spell duration index (CSDI). 2). To capture extremes which have an impact on society and infrastructure; for example, extreme indices like TXge35, CSDI, and WSDI have large impacts on health (Zivin and Shrader, 2016), whereas indices like Rx1day, DTR, CDD, and CWD have large impacts on agriculture and water resources and the economy (Tabari, 2020; Pei et al., 2021).

We use the overlapping periods between N1.0 and N1.5 to compare bias and future projections, i.e., 1990–2009 is used to assess bias between N1.0/N1.5 and observation; and 1990–2009 and 2060–2079 are used for future projections. Since N1.5 historical simulations were available until 2005, we take the remaining four years (2006–2009) from RCP8.5 simulations noting there are minimal differences between all RCP future scenarios for this period.

Some widely used metrics such as bias, root mean square error (RMSE) and spatial correlation (R) are used to quantify the performance for each simulation and ensemble means.

When assessing future changes (compared to historical period) and biases (compared to AGCD observations) in climate extremes we calculate the statistical significance for each grid cell using t-test ($\alpha = 0.05$) assuming equal variance. Results on ensemble mean statistical significance were then separated into three classes following Tebaldi et al. (2011) to identify regions of statistically significant change with model agreement. This method considers the presence of internal climate variability and assesses the degree of consensus between models on the significance of a change. For each grid cell, when 50% or more of the model ensemble (of which there are 12 members in N1.0, 6 members in N1.5 and 18 members in combined ensemble N1.0+N1.5 (hereafter N1.X) show significant change and at least 80% of those models agree on the direction of change, the difference in that grid cell is considered significant (indicated with stippling in the figures). If at least 50% of the model ensemble shows significant change, but less than 80% of those models agree on the direction of change, the multi-model mean is not shown in the subsequent figures but instead the grid cell is shown in white, indicating model disagreement on the projected change. Finally, if less than 50% of the model ensembles show a significant change, we show the multi-model mean in the subsequent figures but without indication of significance (no stippling).

We assess future changes and biases at annual time scale for all extremes, and seasonal time scale for those extremes available at monthly scale. The four seasons are summer (December-January-February, DJF), autumn (March-April-May, MAM), winter (June-July-August, JJA) and spring (September-October-November, SON) in the Southern Hemisphere.

3. Results

3.1. Comparison of N1.0 and N1.5 for historical period (1990–2009)

The main analyses in this section describe the ensemble mean bias in N1.0 and N1.5 with respect to observations for the 12 selected precipitation and temperature extremes. We compare climate indices at annual and seasonal scales. Maps of seasonal mean biases and the absolute values of these variables in the individual N1.0 and N1.5 simulations are available in the supplementary material (Figs. S1-7 and Tables S3–5).

3.1.1. Precipitation related climate extremes

The strongest precipitation extremes are observed at the annual

Table 2
List of ET-SCI Indices evaluated in these study.

No	Index	Definition	Units	Timescale	Sectors
1.	**R99p**	**Total annual precipitation from very heavy precipitation days (Annual sum of daily precipitation > 99th percentile)**	mm	Annual	Coasts
2.	**CWD**	**Consecutive wet days (Maximum annual number of consecutive wet days (when precipitation >= 1.0 mm))**	days	Annual	Coasts
3.	**CDD**	**Consecutive dry days (Maximum number of consecutive dry days (when precipitation < 1.0 mm))**	days	Annual	Health, agriculture and food security, water resources and food security, disaster risk reduction, forestry/GHGs
4.	**R10mm**	**Days when precipitation is at least 10 mm**	days	Annual/ Monthly	Coasts
5.	**Rx1Day**	**Amount of precipitation from very wet days (Maximum 1-day precipitation)**	mm	Annual/ Monthly	Agriculture and food security, water, coasts, disaster risk reduction, forestry/GHGs
6.	**PRCPTOT**	**Total wet-day precipitation (Sum of daily precipitation >= 1.0 mm)**	mm	Annual/ Monthly	Agriculture and food security, water, water resources and food security, forestry/GHGs
7.	**CSDI**	**Cold spell duration indicator (Annual number of days contributing to events where 6 or more consecutive days experience minimum temperature < 10th percentile)**	days	Annual	Health, agriculture and food security, coasts, disaster risk reduction, energy, fisheries, forestry/GHGs, cryosphere
8.	**WSDI**	**Warm spell duration indicator (Annual number of days contributing to events where 6 or more consecutive days experience maximum temperature > 90th percentile)**	days	Annual	Health, agriculture and food security, water resources and food security, coasts, disaster risk reduction, energy, fisheries, forestry/GHGs, cryosphere
9.	**DTR**	**Average range of maximum and minimum temperature**	°C	Annual/ Monthly	Forestry/GHGs
10.	**TXge35**	**Number of days when maximum temperature >= 35 °C**	days	Annual/ Monthly	Health, agriculture and food security, disaster risk reduction, energy, forestry/GHGs
11.	**TXx**	**Warmest daily maximum temperature**	°C	Annual/ Monthly	Agriculture and food security, energy, forestry/GHGs, cryosphere
12.	**TNn**	**Coldest daily minimum temperature**	°C	Annual/ Monthly	Agriculture and food security, energy, forestry/GHGs, cryosphere

timescale and in the summer (DJF) season. For the wet precipitation extremes (PRCPTOT, Rx1Day, R10mm, CWD, and R99p), higher values are mostly observed along the eastern coastal regions of the domain, where most of the Australian population resides (Fig. 3 a-d, f). For the dry precipitation extreme (CDD), higher values are observed inland over the north-west part of the domain (Fig. 3e). In addition to the eastern coastal regions, high elevation regions (Great Dividing Range in south-eastern Australia) also receive high extreme precipitation for R10mm, Rx1Day and PRCPTOT (Figs. S1–3).

Both N1.0 and N1.5 capture the spatial patterns of observed precipitation extremes well (Table S5); however, both tend to overestimate wet extremes (R99p, CWD, R10mm, Rx1Day and PRCPTOT) along the Great Dividing Range (Fig. 3g-j, 3m-p, 3l, 3r), and underestimate dry extreme (CDD) inland (Fig. 3k, q).

In N1.0, CSIRO-MK-3.0 and MIROC3.2 driven simulations show the largest overestimation for wet extreme and underestimation of dry extremes, in contrast, the CCCMA3.1 driven simulations are closest to the observation (Tables S3–4). Similarly, CanESM2 driven simulations and ACCESS1.3 driven R2 simulation generally have smaller biases and RMSEs than other simulations in N1.5 (Tables S3–4). In the same GCM-driven simulations, R2 generally has smaller bias than R1 and R3 simulations in N1.0, and R1 simulation in N1.5, especially for R99p, R10mm, Rx1Day, and PRCPTOT (Tables S3–4).

Overall, the ensemble means for N1.5 perform better than N1.0 for all wet extremes in capturing the spatial patterns of the precipitation extremes (Fig. 3, Table S5). During the wettest (DJF) season the biases of R10mm, Rx1Day and PRCPTOT in N1.5 are substantially smaller than those in N1.0 (Figs. S1–3). This also leads to small annual biases (Fig. 3).

3.1.2. *Temperature related climate extremes*

For the temperature extremes, higher values are mostly observed in inland Australia and over the north-western part of the domain (Fig. 4). The strongest temperature extremes are observed in Summer (DJF) (Figs. S5–7) except for DTR (Fig. S4). All simulations generally capture the spatial pattern of observed temperature extremes well, however, there is large variation in sign and magnitude of biases among the different simulations, seasons and for different temperature extremes (Tables S3–4).

Both N1.0 and N1.5 ensemble means show similar biases (~2–3 days) in magnitude for WSDI and CSDI, however, there are differences in the sign of bias for WSDI (Fig. 4k, q). Most of the N1.0 ensemble members (except for the ECHAM5 driven simulations) show cold biases in WSDI, whereas N1.5 ensemble members show slight warm bias (Table S3). In contrast, the pattern of biases for CSDI are similar between N1.0 and N1.5 for ensemble mean (Fig. 4l, r) and individual simulations (Table S5).

Both N1.0 and N1.5 underestimate annual ensemble means of DTR by ~ 1–3 °C over most of the domain (Fig. 4i, o). The strongest seasonal biases (>5 °C) are observed in autumn (MAM) and winter (JJA) seasons (Fig. S4). Biases in CCCMA3.1 driven simulations are generally smaller than others in N1.0 and ACCESS1.0 driven simulations have slightly larger biases in N1.5 (Tables S3–4).

For TXge35, a cold bias is present for both NARCliM ensembles

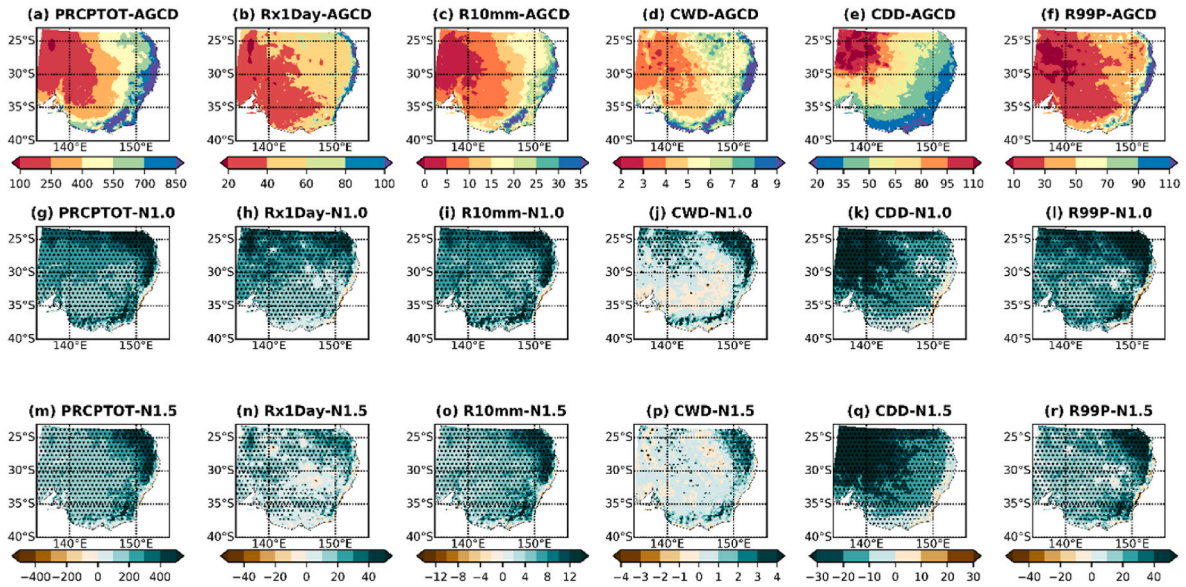

Fig. 3. Climatological mean biases of six precipitation related extremes relative to the Australian Gridded Climate Data dataset (AGCD; top panel a–f), the N1.0 ensemble mean (central panel g–i), N1.5 ensemble mean (bottom panel m–r) at the annual timescale. Data span 1990–2009. Stippling indicates statistically significant differences using a student's t-test at the 95% confidence level.

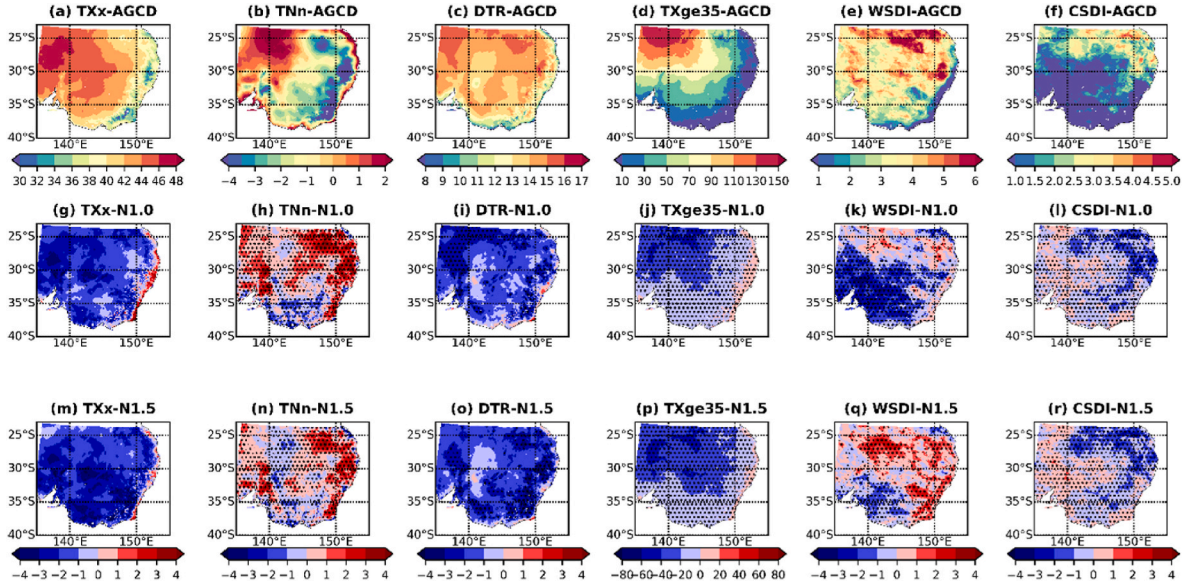

Fig. 4. Climatological mean biases of six temperature related extremes relative to the Australian Gridded Climate Data dataset (AGCD; top panel a–f), the N1.0 ensemble mean (central panel g–i), N1.5 ensemble mean (bottom panel m–r) at the annual timescale. Data span 1990–2009. Stippling indicates statistically significant differences using a student's t-test at the 95% confidence level.

(Fig. 4j, p). At the annual timescale, except for CCCMA3.1 and ECHAM5 driven N1.0 simulations, all the other simulations show a strong underestimation of ~50 days over the northwest of the domain and small bias ~10 days along the coastal regions (Not shown). In contrast, CCCMA3.1 and ECHAM5 driven N1.0 simulations show overestimation in the north-eastern part of the domain and underestimation in the northwest domain. A similar underestimation can be observed across N1.5 simulations (Tables S3–4). TXge35 itself is the largest in Summer (DJF), the largest underestimation is seen in summer and the smallest in winter (Fig. S5).

For TXx, similar results are observed as TXge35 (Tables S3–4). Here, except for CCCMA3.1 and ECHAM5 driven N1.0 simulations, all other simulations show cold biases in TXx. CCCMA3.1 and ECHAM5 driven N1.0 simulations show slight warm bias in the north-eastern part of the domain. Bias in TXx for the ACCESS1.0-driven simulations is slightly larger than other simulations in N1.5. On average, similar biases are evident in N1.0 and N1.5 ensemble (Fig. 4g, m). Bias in TXx for each season is similar with small warm bias along southeast coastal region and cold bias inland (Fig. S6).

For TNn, both N1.0 and N1.5 ensembles show similar warm bias (~1–2 °C) at the annual timescale (Fig. 4h, n). Seasonal biases are larger, especially for autumn and winter seasons with more than 2 °C warm bias, whereas both generally show a cold bias (~2–3 °C) in summer and spring seasons (Fig. S7). All simulations in N1.0 and N1.5 have similar pattern and magnitude of bias (Tables S3–5).

In general, the ensemble means for N1.5 are similar to N.10 for all temperature extremes in capturing the spatial patterns of the temperature extremes. Both N1.0 and N1.5 underestimate hot extremes (TXx and

TXge35) and daily temperature range, and overestimate cold extreme (TNn).

3.2. Domain averaged results

To compare the domain-averaged results for N1.0 and N1.5, Taylor diagrams (Taylor 2001) for model evaluation are examined. Taylor diagrams provide a concise statistical summary of how well patterns match each other in terms of their correlation, their root-mean-square error (RMSE) and the ratio of their variances. The Taylor Diagram indicates the baseline observed point where correlation is 1 and RMSE equals 0. If the simulation point is close to the observed point, it means that they are similar in terms of standard deviation, their correlation is high, and their RMSE is close to zero.

In this section, we evaluate and compare domain averaged climate extremes for each N1.0 and N1.5 simulations and their seasonal (where applicable) and annual ensemble means.

3.2.1. Precipitation related climate extremes

For R99p (Fig. 5a) and Rx1Day (Fig. 6) high correlations (r ~ 0.7) are observed between observations and N1.X ensemble members. For both the indices, small differences are observed between the correlations and standard deviation for individual N1.X ensemble members. Weak correlations (r = 0.3–0.5) are observed for all the other extreme precipitation indices (CWD, CDD, R10mm and PRCPTOT) (Figs. 5 and 6). For R10mm and PRCPTOT, N1.5 ensemble members are consistently closer to observations for DJF and MAM seasons (Fig. 6). For these indices, N1.0 simulations on average show a large spread and standard deviations for the CSIRO-MK3.0 driven simulations. For CWD, N1.5 ensemble members show a large spread and standard deviations for the CanESM2 driven simulations.

3.2.2. Temperature related climate extremes

For WSDI and CSDI (Fig. 7) moderate to weak correlations (r ~ 0.4–0.5) are observed between observations and individual N1.X ensemble members. Also, for these indices, NARCliM ensemble members show large variability from the observations. For all other temperature extremes (DTR, TXge35, TXx and TNn) all ensemble members show strong correlations (r > 0.8) with the observations (Fig. 8). In addition to strong correlations, ensemble members show small variability between themselves and observations.

3.3. Comparison of future projections in climate extremes

Having assessed the performance of N1.5 simulations in comparison to the N1.0 ensemble members and observations for the historical period (1990–2009), we now focus on comparing N1.0 and N1.5 for the future projections. N1.5 has two overlapped future periods with N1.0, here we focus on the far future (2060–2079) to compare future projections in 12 precipitation and temperature related extremes. As described earlier, N1.5 is designed to complement N1.0 simulations, therefore N1.X includes a wider range of plausible future changes in precipitation and temperature of CMIP3 and CMIP5 ensemble (Fig. 2). For this reason, here we present future projections from N1.0, N1.5 and the combined N1.X ensembles.

3.3.1. Precipitation related climate extremes

Changes in six annual precipitation extremes for the far future are presented in Fig. 9. The N1.5 ensemble projects quite different changes in precipitation extremes from the N1.0 ensemble, even if there are some spatial similarities for each extreme.

N1.0 projects significant increases in R99p for the whole domain, especially a larger increase for eastern regions along the Great Dividing Range (Fig. 9f). The large increase in R99p in N1.0 projection is mainly caused by three MIROC3.2-driven simulations which project more than 60% increase in R99p (Table S6). In contrast, N1.5 project much smaller increase in R99p for the region along the Great Diving Range and decrease for most of the inland (Fig. 9l). All N1.5 simulations project similar magnitude of changes in R99p, with most simulations projecting an increase over Great Dividing Range (Table S6).

Both N1.0 and N1.5 ensembles generally show future decreases in annual mean CWD (Fig. 9d, j) throughout the domain, especially for Victoria, although the changes are not significant for both ensembles. Large decreases in projected CWD in Victoria can be seen in most of N1.0 simulations, except for the three ECHAM5 driven simulations. Similarly, decreases in CWD for the N1.5 ensemble mean are mostly determined by ACCESS1.3-driven simulations and ACCESS1.0-driven R2 (Table S6). For annual CDD (Fig. 9e, k), both N1.0 and N1.5 ensemble means show future increases over most of the domain. However, the increases in N1.5 ensemble mean are stronger when compared to N1.0 ensemble

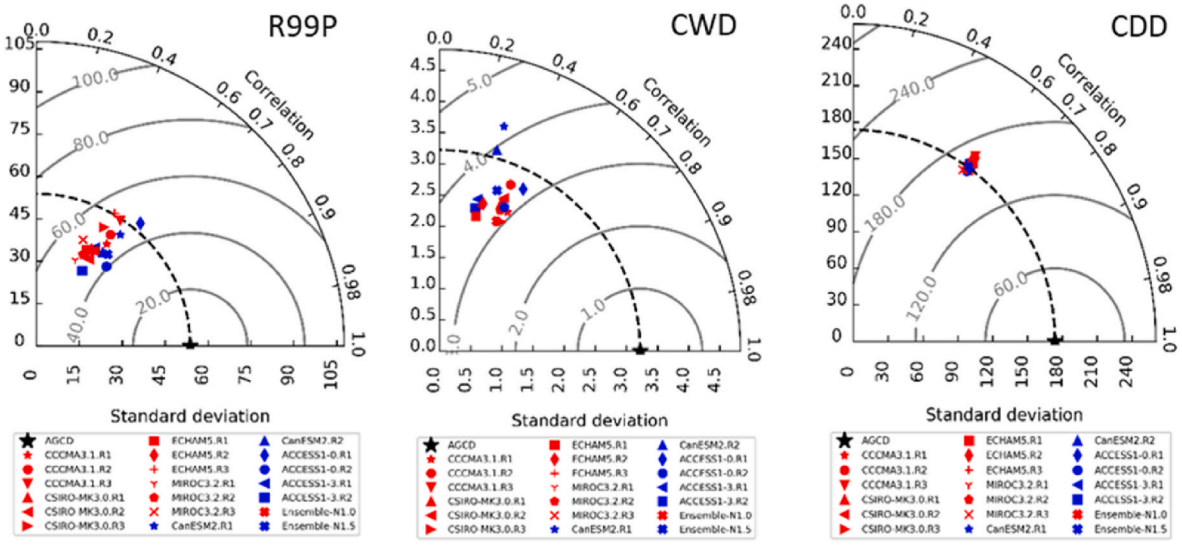

Fig. 5. Taylor diagrams comparing climatological mean R99p (left), CWD (central) and CDD (right) to the reference Australian Gridded Climate Data (AGCD) dataset at an annual timescale. Horizontal and vertical axes represent the spatial standard deviation; the outer circle represents the pattern correlation between each ensemble member and the reference dataset (AGCD); and the grey circles radiating from the bottom indicate centred root mean square errors. Models closer to the black star indicate a closer match to the reference dataset. Data spans 1990—2009.

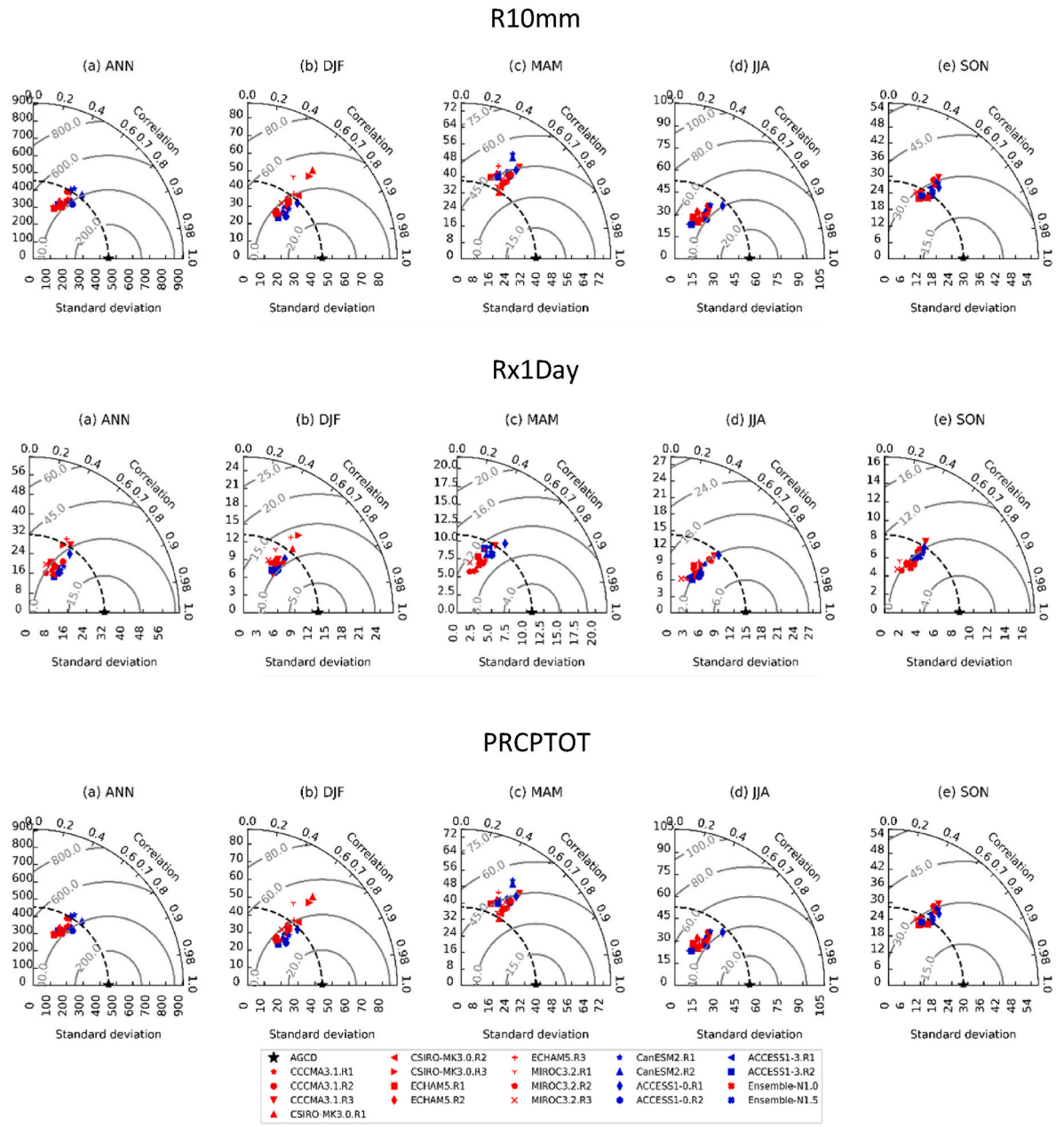

Fig. 6. Taylor diagrams comparing climatological mean R10mm (top), Rx1Day (central) and PRCPTOT (bottom) to the reference Australian Gridded Climate Data (AGCD) dataset: annual (panel a), December-January-February (panel b), March-April-May (panel c), June-July-August (panel d) and September-October-November (panel e). Horizontal and vertical axes represent the spatial standard deviation; the outer circle represents the pattern correlation between each ensemble member and the reference dataset (AGCD); and the grey circles radiating from the bottom indicate centred root mean square errors. Models closer to the black star indicate a closer match to the reference dataset. Data spans 1990—2009.

mean. Also, CCCMA3.1- and MIROC3.2-driven simulations show future decreases in CDD (Table S6).

Like R99p, N1.0 ensemble mean projects increases in Rx1Day for most of the domain (Fig. 9b). Significant increases in Rx1Day in Summer and Autumn contribute to the annual change, in contrast, there is little change in R1xDay in winter and spring (Fig. S8). The increase in Rx1Day in N1.0 is mostly attributable to the three MIROC3.2-driven simulations (Table S6). N1.5 projects slightly increases and decreases in Rx1Day for the eastern and inland regions, respectively. The increase in Rx1Day is mostly in Summer, and decrease is in other seasons, especially in Spring (Fig. S8).

N1.0 ensemble mean projects similar future changes in R10mm and PRCPTOT (Fig. 9a, c), i.e. Decrease is in Victoria and increase elsewhere. The decrease is mostly in Spring but increase in Summer and Autumn (Figs. S9–10). The decrease can be observed in all N1.0 simulations even for MIROC3.2- and CCCMA3.1-driven simulations that project large increase in northern domain (Table S6). Similarly, N1.5 also projects similar decrease in R10mm and PRCPTOT (Fig. 9g, i). Similar to N1.0, the decrease is mostly in Spring (Figs. S9–10), which is mostly contributed by two ACCESS1.3-driven simulations and ACCESS1.0-driven R2 simulation (Table S6).

N1.X projection covers the whole future change space of CMIP3 and CMIP5 (Fig. 2), which projects drier future ie. less annual total precipitation (Fig. 9m), shorter wet period and longer dry period (Fig. 9p and q), and fewer days with more than 10 mm daily precipitation (Fig. 9o), however it projects larger Rx1Day and R99p (Fig. 9n and r). This implies that precipitation events will become more intense under the future climate conditions.

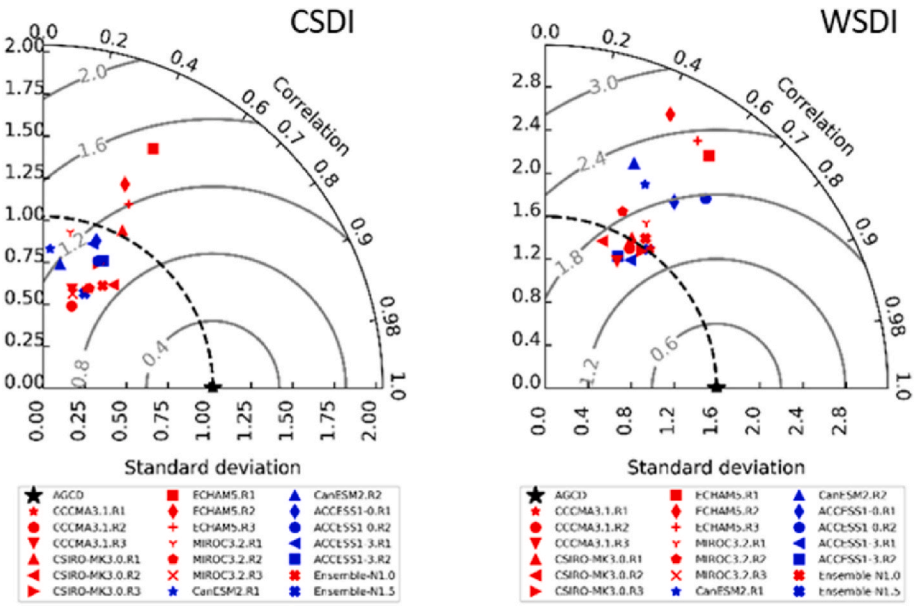

Fig. 7. Taylor diagrams comparing climatological mean CSDI (left) and WSDI (right) to the reference Australian Gridded Climate Data (AGCD) dataset at an annual timescale. Horizontal and vertical axes represent the spatial standard deviation; the outer circle represents the pattern correlation between each ensemble member and the reference dataset (AGCD); and the grey circles radiating from the bottom indicate centred root mean square errors. Models closer to the black star indicate a closer match to the reference dataset. Data spans 1990—2009.

3.3.2. *Temperature related climate extremes*

In contrast to projections of precipitation extremes, N1.0 and N1.5 generally project similar changes in temperature extremes, especially for TNn, TXge35, WSDI and CSDI (Fig. 10).

Both N1.0 and N1.5 project future decreases (1–2 days) in annual mean CSDI (Fig. 10f, l). This is expected because of the consistent future increases in mean temperature. The strongest decrease in CSDI is projected in the northern part of the domain. ECHAM5-driven N1.0 simulations, and ACCESS1.0- and ACCESS1.3-driven N1.5 simulations project the strongest future decreases in CSDI (Table S6). In contrast, both N1.0 and N1.5 project strong future increases in WSDI (~30–50 days) (Fig. 10e, k). N1.5 ensemble members generally show larger projected increases in annual mean WSDI than N1.0, which is likely due to hotter GCMs used in N1.5 simulations than those in N1.0. All simulations in N1.0 and N1.5 generally project similar pattern of future changes with larger increase in northern domain and along Great Dividing Range (Not shown).

For DTR, stronger future changes are projected in the spring (September-October-November) for N1.0 (Fig. S11). However, N1.5 ensemble mean, and individual simulations show future increases in DTR, even if the simulated changes are not statistically significant (Fig. S11).

Both N1.0 and N1.5 project strong future increase in TXx and TNn both annually (Fig. 10 a, g, b, h) and for all seasons (Figs. S12–13). The projected changes are typically stronger for TXx (~3–4 °C) than for TNn (~1–2 °C), however, changes in TXx are not statistically significant (Fig. S12). In contrast, both TNn ensemble mean and each simulation in N1.0 and N1.5 project significant increase (Fig. S13).

For TXge35, both N1.0 and N1.5 show strong future increases (Fig. 10d, j). The strongest increases are projected in Summer and the weakest increases in winter (Fig. S14). All simulations in N1.0 and N1.5 project similar change pattern with larger increase in the northern domain (Not shown).

Generally, N1.5 projects stronger changes in temperature extremes than N1.0. This can be partially attributed to hotter CMIP5 GCMs used in N1.5 (Fig. 2). Meanwhile, simulations which project larger increases/decreases in precipitation extremes, also generally project smaller/larger increases in temperature extremes.

Overall, N1.X projects longer warm (WSDI) and shorter cold (CSDI) periods, higher maximum and minimum temperature (TXx, TNn), more extreme hot days (TXge35), and larger daily temperature range (DTR).

4. Discussion

In this study, we evaluated 12 climate extremes for the N1.0 and N1.5 ensembles. The evaluation indicates both N1.0 and N1.5 overestimate wet climate extremes, especially for inland Australia and along Great Dividing Range in eastern Australia. In contrast they significantly under-estimate dry climate extremes. We also observed that, for some temperature related extremes such as TXx, DTR, TXge35, both N1.0 and N1.5 show strong cold biases.

As discussed in Nishant et al. (2021), wet and cold bias in N1.0 and N1.5 simulations might be related to the unified Noah land surface scheme used in those simulations (Olson et al., 2016; Ji et al., 2016). The unified Noah land surface scheme often overestimates soil moisture (Zhou et al., 2019), which results in more evapotranspiration over land surface that leads to more rainfall and a cooler surface (Liu and Pu, 2019). As a part of future work, we have included other land surface models such as Noah-MP and CLM in the selection of RCMs for the third generation of NARCliM (N2.0) (Di Virgilio et al., in preparation), which will overcome most of the limitation of the combined N1.0 and N1.5 ensemble.

Previously, strong negative correlations were observed between mean monthly precipitation biases and mean monthly maximum temperature biases across Australia, including the present study area (Di Virgilio et al., 2019a). This could suggest overestimation in wet extremes is a likely cause of the large cold bias in some temperature extremes. Multiple studies have indicated that some of the precipitation biases in N1.0 simulations are inherited from the driving GCMs (Di Luca et al., 2016a; Olson et al., 2016). Another reason for wet biases in N1.0 and N1.5 simulations can be related to different physics schemes used in the WRF model. Our results show that R2 simulation generally has much smaller biases than R1 (used in N1.0 and N1.5) and R3 (used in N1.0 only) for multiple wet extremes such as R99p, Rx1Day, and PRCPTOT.

Some uncertainties in observations might also contribute to the biases in the results. The observation AGCD was interpolated from the unevenly distributed weather monitoring sites. There are substantially fewer monitoring sites over the Great Dividing Range and inland areas, which result in large uncertainties in estimated observed precipitation over those areas. Chubb et al. (2016) used an independent gauge network to evaluate AGCD precipitation over Australian Snowy Mountains (part of Great Dividing Range) and identified that daily precipitation is under-estimated by at least 15%. This suggests that the true biases in N1.0 and N1.5 over the Great Dividing Range may be smaller

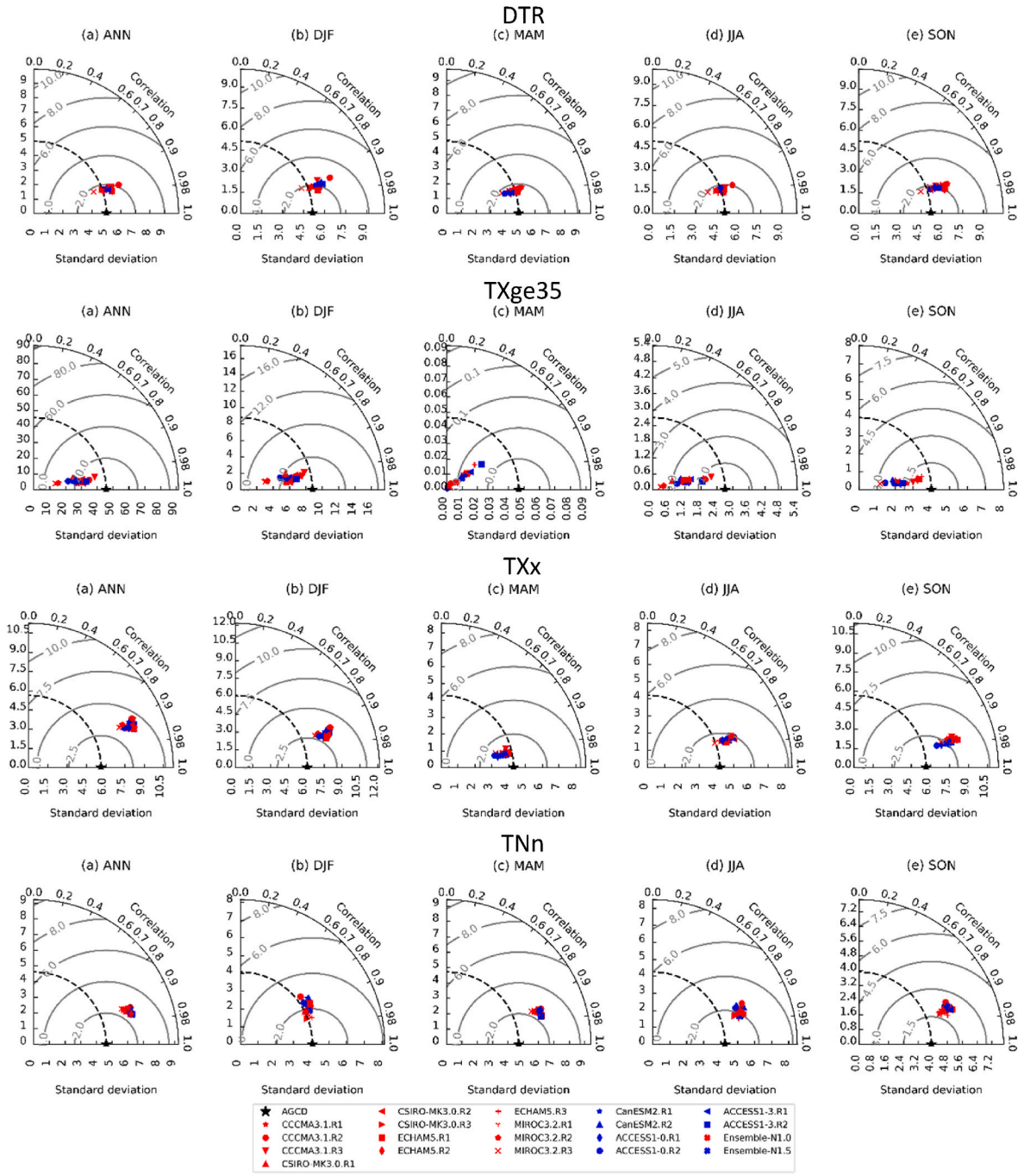

Fig. 8. Taylor diagrams comparing climatological mean DTR, TXge35, TXx, and TNn to the reference Australian Gridded Climate Data (AGCD) dataset: annual (panel a), December-January-February (panel b), March-April-May (panel c), June-July-August (panel d) and September-October-November (panel e). Horizontal and vertical axes represent the spatial standard deviation; the outer circle represents the pattern correlation between each ensemble member and the reference dataset (AGCD); and the grey circles radiating from the bottom indicate centred root mean square errors. Models closer to the black star indicate a closer match to the reference dataset. Data spans 1990—2009.

than presented here. Similarly, for the north-western inland area, using limited gauge stations to generate gridded data might miss many extreme precipitation events, which are often localized.

In terms of comparisons between N1.0 and N1.5, the wet climate extremes simulated in N1.5 show smaller biases than N1.0, especially in Summer. The dry extreme (CDD) and temperature extremes in N1.5 generally show comparable results with N1.0. The smaller bias in N1.5 simulations is again attributed to the driving GCMs in N1.5 simulations, most of which show smaller biases than the driving GCMs in N1.0 simulations. Available studies have suggested that the finer scales of the CMIP5 GCMs leads to more accurate estimation of precipitation than CMIP3 models (Gulizia and Camilloni, 2015). It has always been a challenging task for models to simulate precipitation accurately (Li et al., 2016; Potter et al., 2020). N1.5 simulations show a substantial improvement in capturing the seasonal patterns and magnitudes of precipitation extremes. These results indicate that N1.5 simulations are an improvement on the earlier N1.0 in simulating the historical climate, at least for precipitation extremes.

Future projections of precipitation extremes in N1.0 and N1.5 simulations show contrasting results. These major differences can be partly

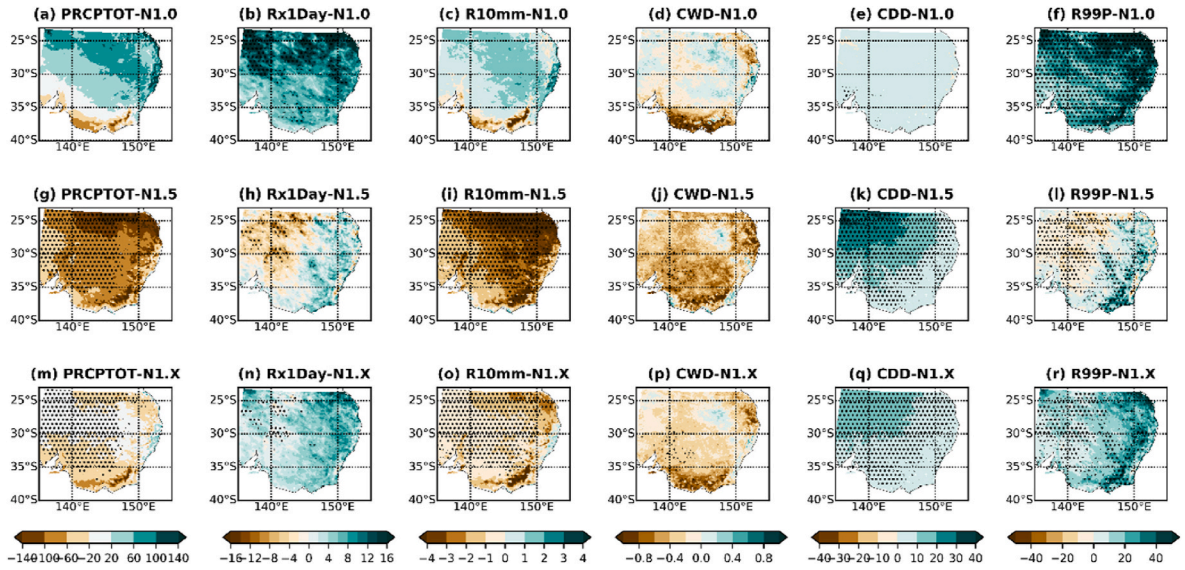

Fig. 9. Change in annual climatological mean precipitation extremes between 1990—2009 and 2060—2079. Future time periods are based on the SRESA2 and RCP8.5 emission scenarios for N1.0 and N1.5, respectively. The N1.0 ensemble mean change (top panel a–f), N1.5 ensemble mean change (central panel g–i), and N1.x ensemble mean change (bottom panel m–r). Stippling indicates statistically significant change using a student's t-test at the 95% confidence level.

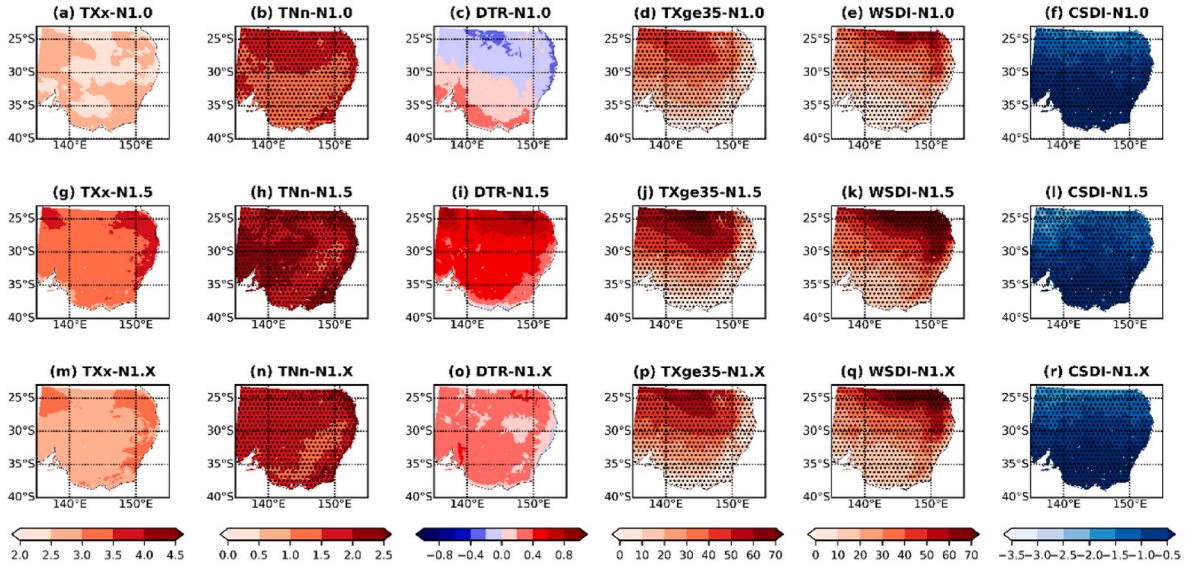

Fig. 10. Change in annual climatological mean temperature extremes between 1990—2009 and 2060—2079. Future time periods are based on the SRESA2 and RCP8.5 emission scenarios for N1.0 and N1.5, respectively. The N1.0 ensemble mean change (top panel a–f), N1.5 ensemble mean change (central panel g–i), and N1.x ensemble mean change (bottom panel m–r). Stippling indicates statistically significant change using a student's t-test at the 95% confidence level.

explained by the driving GCMs in N1.0 and N1.5 simulations. The ensemble mean of CMIP5 GCMs in N1.5 is drier than that of CMIP3 GCMs in N1.0 (Fig. 2), which result in much smaller increase or even decrease in wet extremes in N1.5 precipitation extreme projections. The spatial patterns of future changes in temperature extremes are found to be comparable in N1.5 and N1.0 simulations. Both sets of simulations project future warming throughout the domain, however the magnitude of changes in temperature extremes is found to be stronger in N1.5 simulations. This is understandable, as CMIP5 GCMs used in N1.5 simulations are hotter than those CMIP3 GCMs in N1.0 (Fig. 2).

This paper also presented combined results of N1.0 and N1.5 (N.1X) for the future climate extreme projections. N1.X projections demonstrate the complementary utility of N1.5 with the original N1.0 and the underlying objective that N1.5 simulations do not replace N1.0 simulations, rather, these updated and enhanced simulations complement N1.0 simulations by expanding the future change space covered by the simulations. Compared to CMIP3 GCMs, a number of CMIP5 GCMs projected a hotter and drier future expanding the future change space of the CMIP3 GCMs (Fig. 2). Together N1.0 and N1.5 provide a more complete sampling of this combined future change space. However, it should be noted that N1.0 and N1.5 are driven by GCMs from different generation of CMIP, and emission scenarios used in N1.0 and N1.5 are not the same. There is constraint/limitation when N1.0 and N1.5 are combined as N1.x.

These projected results suggest more intense climate extremes in the future. The findings are aligned with other studies. For an example, Bao et al. (2017) used NARCliM1.0 to assess future changes in extreme precipitation and found future increase in extreme precipitation exceed observed scaling rate. Other studies also confirmed that changes in extreme precipitation is much larger than 7% per degree warming

(Fischer and Knutti, 2015). Therefore adaptation, resilience and mitigation strategies must anticipate these plausible changes in future climate extremes. For example, significant increase in hot extremes will enlarge heatwave exposure for Australian especially for elderly population (Nishant et al., 2022). The future projections of hot extremes are critical for planning where adaption measures might be necessary to copy with heatwave exposure such as improvements in infrastructure including housing and air conditioning, together with socioeconomic changes and better health care and service. Significant increase in CDD (consecutive dry days) and decrease in CWD (consecutive wet day) together with higher temperature are expected to exacerbate the pressure on food production. Projection of climate extremes are important for agricultural predictions and adaptation planning, which provides an overview of critical regions that are most susceptible to variations in growing season climate and climate extremes (Vogel et al., 2019). Increase in extreme rainfall will significantly impact rainfall erosivity that can cause substantial hillslope erosion and land degradation (Zhu et al., 2019). The projections of rainfall extremes will help to take necessary adaption measures to minimise the impacts such as land use planning and development of cost-effective erosion control practices.

The uncertainties from emission scenarios and GCMs can be reduced by dynamically downscaling GCMs but cannot be totally removed (Ning et al., 2012). Some uncertainties are also attributable to RCMs and parameterizations within the models. Therefore, we would like to remind readers to be aware of the uncertainties in the study when they use projections to undertake impact assessments and future planning.

Understanding the dynamics/thermodynamic components behind future changes in climate extremes is limited. Some studies indicated changes in precipitation extremes are possibly due to changes in synoptic patterns and available moisture (Bao et al., 2017; Li et al., 2018), poleward shift of subtropic ridge and SAM (Southern Annual Modes) might cause more temperature extremes such as heatwaves (Perkins-Kirkpatrick et al., 2016). Relationships between some climate extremes and large-scale and synoptic variability have been identified. However, more research is required to further our understanding of the dynamical interactions of climate extremes.

5. Conclusions

This paper evaluates and compares skills of 12 simulations in NARCliM1.0 and six simulations in NARCliM 1.5 to capture 12 precipitation and temperature extremes for Southeast Australia. The results of this study show that N1.5 ensemble is better in capturing the spatial patterns of precipitation extremes than N1.0. Biases of R10mm, Rx1Day and PRCPTOT in N1.5 are substantially smaller than those in N1.0, especially during summer. Overall, ensemble means for N1.5 are similar to N1.0 for temperature extremes. Both ensembles underestimate hot extremes (TXx and TXge35) and daily temperature range but overestimate cold extremes (TNn).

This paper also presents future projections of 12 climate extremes for N1.0 and N1.5 under high emissions scenarios. We show that N1.0 and N1.5 project different spatial patterns of future changes in precipitation extremes but similar patterns of changes in temperature extremes. Those differences in climate extremes between N1.0 and N1.5 are partially related to differences between the driving GCMs. The combined future projections of both N1.0 and N1.5 (N1.X) are also provided, which provides a more complete sampling of the future change space. However, there are some limitations of combining CMIP3 SRES A2 and CMIP5 RCP8.5 projections due to variations in the driving emissions.

N1.X projects drier future: i.e., less annual total precipitation (PRCPTOT), shorter wet period (CWD) and longer dry period (CDD), and fewer days with more than 10 mm daily precipitation (R10mm), however, it projects larger R99p and Rx1Day. N1.X also projects hotter future, ie. longer warm period (WSDI) and shorter cold period (CSDI), higher maximum and minimum temperature (TXx, TNn), more extreme hot days (TXge35), and larger daily temperature range (DTR). This implies that precipitation and temperature extremes will get more intensive under the future drier and hotter conditions.

The results of this study have broad implications for important decision-making processes in the context of climate change adaptation. The outcomes of this work form a baseline for short-, medium- and long-term responses to climate extremes and the facilitation of effective and responsive climate-resilient planning across south-east Australia.

Credit author statement

Ji, Fei: Conceptualization, Methodology, Formal analysis, Investigation, Validataion, Writing original draft, Writing-Review & Editing. Nishant, Nidhi: Conceptualization, Methodology, Software, Validation, Formal analysis, Visualization, Writing original draft, Writing-Review & Editing. Evans, Jason P.: Methodology, Investigatioin, Writing-Review & Editing. Di Virgilio, Giovanni: Investigation, Writing-Review & Editing. Cheung Kevin K. W.: Investigation, Writing-Review & Editing. Tam, Eugene: Software, Data Curation, Investigation, Writing-Review & Editing. Beyer, Kathleen: Supervision, Project Administration, Funding acquisitation, Investigation, Writing-Review & Editing. Riely, Matthew L.: Supervision, Project Administration, Funding acquisitation, Investigation, Writing-Review & Editing.

Declaration of competing interest

The authors declare that they have no known competing financial interests or personal relationships that could have appeared to influence the work reported in this paper.

Data availability

Data will be made available on request.

Acknowledgments

This work is made possible by funding from the NSW Climate Change Fund for NSW and Australian Regional Climate Modelling (NARCliM) Project. The modelling work was undertaken on the National Computational Infrastructure (NCI) high performance computers in Canberra, Australia, which is supported by the Australian Commonwealth Government. We thank the climate modelling groups for producing and making available their model outputs, the Earth System Grid Federation (ESGF) for archiving the data and providing access, and the multiple funding agencies who support CMIP3, CMIP5 and the Earth System Grid Federation (ESGF).

J. P. Evans acknowledges the support of the Australian Research Council Centre of Excellence for Climate Extremes (CE170100023) and the Climate Systems Hub of the Australian Governments National Environmental Science Program.

Appendix A. Supplementary data

Supplementary data to this article can be found online at https://doi.org/10.1016/j.wace.2022.100526.

References

Alexander, L.V., Arblaster, J.M., 2017. Historical and projected trends in temperature and precipitation extremes in Australia in observations and CMIP5. Weather Clim. Extrem. 15, 34–56.

Alexander, L.V., Herold, N., 2015. Climpactv2 indices and software. A document prepared on behalf of the commission for climatology (CCL) Expert Team on sector-specific climate indices (ET-SCI). Retrieved from. https://epic.awi.de/id/eprint/49274/1/ClimPACTv2_manual.pdf.

Argüeso, D., Evans, J.P., Fita, L., Bormann, K.J., 2014. Temperature response to future urbanization and climate change. Clim. Dynam. 42 (7–8), 2183–2199.

Argüeso, D., Evans, J.P., Pitman, A.J., Di Luca, A., 2015. Effects of city expansion on heat stress under climate change conditions. PLoS One 10 (2), e0117066.

Ayugi, B., Jiang, Z., Zhu, H., Ngoma, H., Babaousmail, H., Karim, R., Dike, V., 2021. Comparison of CMIP6 and CMIP5 models in simulating mean and extreme precipitation over East Africa. Int. J. Climatol. 41, 6474–6496. https://doi.org/10.1002/joc.7207.

Bao, J., Sherwood, S.C., Alexander, L.V., Evans, J.P., 2017. Future increases in extreme precipitation exceed observed scaling rates. Nat. Clim. Change 7 (2), 128–132.

Cheneka, B.R., Brienen, S., Frohlich, K., Asharaf, S., Fruh, B., 2016. Searching for an added value of precipitation in downscaled seasonal hindcasts over east africa: COSMO-CLM forced by MPI-ESM. Adv. Meteorol. 2016, 4348285.

Choudhary, A., Dimri, A.P., Paeth, H., 2019. Added value of CORDEX-SA experiments in simulating summer monsoon precipitation over India. Int. J. Climatol. 39, 2156–2172.

Chubb, T.H., Manton, M.J., Siems, S.T., Peace, A.D., 2016. Evaluation of the AWAP daily precipitation spatial analysis with an independent gauge network in the Snowy Mountains. J. South. Hemisph. Earth Sys. Sci. 2016 (66), 55–67.

Clarke, H., Evans, J.P., 2019. Exploring the future change space for fire weather in southeast Australia. Theor. Appl. Climatol. 136, 513–527. https://doi.org/10.1007/s00704-018-2507-4.

Clarke, H., Pitman, A.J., Kala, J., Carouge, C., Haverd, V., Evans, J.P., 2016. An investigation of future fuel load and fire weather in Australia. Climatic Change 139 (3–4), 591–605.

Cortés-Hernández, V.E., Zheng, F., Evans, J., et al., 2015. Evaluating regional climate models for simulating sub-daily rainfall extremes. Clim. Dynam. 47, 1613–1628. https://doi.org/10.1007/s00382-015-2923-4.

Dee, D.P., Uppala, S.M., Simmons, A.J., Berrisford, P., Poli, P., Kobayashi, S., Bechtold, P., 2011. The ERA-Interim reanalysis: configuration and performance of the data assimilation system. Q. J. R. Meteorol. Soc. 137 (656), 553–597.

Di Luca, A., de Elía, R., Laprise, R., 2013. Potential for small scale added value of RCM's downscaled climate change signal. Clim. Dynam. 40, 601–618.

Di Luca, A., Argüeso, D., Evans, J.P., de Elía, R., Laprise, R., 2016a. Quantifying the overall added value of dynamical downscaling and the contribution from different spatial scales. J. Geophys. Res. Atmos. 121, 1575–1590.

Di Luca, A., Evans, J.P., Pepler, A., et al., 2016b. Australian east coast lows in a regional climate model ensemble. J. South. Hemisph. Earth Sys. Sci. 66, 108–124.

Di Virgilio, G., Evans, J.P., Blake, S.A.P., et al., 2019. Climate change increases the potential for extreme wildfires. Geophys. Res. Lett. 46, 8517–8526. https://doi.org/10.1029/2019GL083699.

Di Virgilio, G., Evans, J.P., Di Luca, A., Olson, R., Argueso, D., Kala, J., Andrys, J., Hoffmann, P., Katzfey, J.J., Rockel, B., 2019a. Evaluating reanalysis driven CORDEX regional climate models over Australia: model performance and errors. Clim. Dynam. 53, 2985–3005.

Di Virgilio, G., Evans, J.P., Di Luca, A., et al., 2020. Realised added value in dynamical downscaling of Australian climate change. Clim. Dynam. 54, 4675–4692.

Dosio, A., Panitz, H.J., Schubert-Frisius, M., Luthi, D., 2015. Dynamical downscaling of CMIP5 global circulation models over CORDEX-Africa with COSMO-CLM: evaluation over the present climate and analysis of the added value. Clim. Dynam. 44, 2637–2661.

Dosio, A., Jones, R.G., Jack, C., Lennard, C., Nikulin, G., Hewitson, B., 2019. What can we know about future precipitation in Africa? Robustness, significance and added value of projections from a large ensemble of regional climate models. Clim. Dynam. 53 (9–10), 5833–5858.

Ekström, M., Grose, M.R., Whetton, P.H., 2015. An appraisal of downscaling methods used in climate change research. Wiley Interdiscipl. Rev.: Clim. Change 6 (3), 301–319.

Evans, J.P., Ji, F., 2012. Choosing the RCMs to Perform the Downscaling. NARCliM Technical Note 2. NARCliM Consortium, Sydney, Australia, p. 8.

Evans, J.P., Ekström, M., Ji, F., 2012. Evaluating the performance of a WRF physics ensemble over South-East Australia. Clim. Dynam. 39, 1241–1258.

Evans, J.P., Ji, F., Abramowitz, G., Ekström, M., 2013. Optimally choosing small ensemble members to produce robust climate simulations. Environ. Res. Lett. 8, 044050.

Evans, J.P., Ji, F., Lee, C., Smith, P., Argüeso, D., Fita, L., 2014. Design of a regional climate modelling projection ensemble experiment; NARCliM. Geosci. Model Dev. (GMD) 7, 621–629.

Evans, J.P., Argueso, D., Olson, R., Di Luca, A., 2017. Bias-corrected regional climate projections of extreme rainfall in south-east Australia. Theor. Appl. Climatol. 130, 1085–1098.

Evans, J.P., Kay, M., Prasad, A., Pitman, A., 2018. The resilience of Australian wind energy to climate change. Environ. Res. Lett. 13, 024014 https://doi.org/10.1088/1748-9326/aaa632.

Evans, A., Jones, D., Smalley, R., Lellyett, S., 2020. An Enhanced gridded rainfall analysis scheme for Australia. http://www.bom.gov.au/research/publications/researchreports/BRR-041.pdf.

Fischer, E.M., Knutti, R., 2015. Anthropogenic contribution to global occurrence of heavy-precipitation and high-temperature extremes. Nat. Clim. Change 5 (6), 560–564.

Fita, L., Evans, J.P., Argüeso, D., et al., 2016. Evaluation of the regional climate response in Australia to large-scale climate models in the historical NARCliM simulations. Clim. Dynam. 1–15. https://doi.org/10.1007/s00382-016-3484-x.

Flato, G., Coauthors, 2013. Evaluation of climate models. In: Stocker, T.F., et al. (Eds.), Chapter 9 in Climate Change 2013: The Physical Science Basis. Cambridge University Press, pp. 741–866.

Gnitou, G.T., Tan, G.R., Ma, T.H., Akinola, E.O., Nooni, I.K., Babaousmail, H., Al-Nabhan, N., 2021. Added value in dynamically downscaling seasonal mean temperature simulations over West Africa. Atmos. Res. 260 105694.

Gulizia, C., Camilloni, I., 2015. Comparative analysis of the ability of a set of CMIP3 and CMIP5 global climate models to represent precipitation in South America. Int. J. Climatol. 35 (4), 583–595.

Herold, N., Alexander, L., 2016. Climpact 2. https://github.com/ARCCSS-extremes/climpact2.

Herold, N., Downes, S.M., Gross, M.H., Ji, F., Nishant, N., Macadam, I., Ridder, N.N., Beyer, K., 2021. Projected changes in the frequency of climate extremes over southeast Australia. Environ. Res. Commun. 3 https://doi.org/10.1088/2515-7620/abe6b1 (2021) 011001.

Jacob, D., Petersen, J., Eggert, B., Alias, A., Christensen, O.B., Bouwer, L.M., Braun, A., Colette, A., Déqué, M., Georgievski, G., Georgopoulou, E., Gobiet, A., Menut, L., Nikulin, G., Haensler, A., Hempelmann, N., Jones, C., Keuler, K., Kovats, S., Kröner, N., Kotlarski, S., Kriegsmann, A., Martin, E., van Meijgaard, E., Moseley, C., Pfeifer, S., Preuschmann, S., Radermacher, C., Radtke, K., Rechid, D., Rounsevell, M., Samuelsson, P., Somot, S., Soussana, J.-F., Teichmann, C., Valentini, R., Vautard, R., Weber, B., Yiou, P., 2014. EURO-CORDEX: new high-resolution climate change projections for European impact research. Reg. Environ. Change 14, 563–578. https://doi.org/10.1007/s1011.3-013-0499-2.

Ji, F., Ekström, M., Evans, J.P., Teng, J., 2014. Evaluating rainfall patterns using physics scheme ensembles from a regional atmospheric model. Theor. Appl. Climatol. 115, 297–304.

Ji, F., Evans, J.P., Argueso, D., Fita, L., Di Luca, A., 2015. Using large-scale diagnostic quantities to investigate change in East Coast Lows. Clim. Dynam. 45 (9–10), 2443–2453.

Ji, F., Evans, J.P., Teng, J., Scorgie, Y., Argüeso, D., Di Luca, A., 2016. Evaluation of long-term precipitation and temperature Weather Research and Forecasting simulations for southeast Australia. Clim. Res. 67, 99–115.

Ji, F., Evans, J.P., Di Luca, A., Jiang, N.B., Olson, R., Fita, L., Argueso, D., Chang, L.T.-C., Scorgie, Y., Riley, M.L., 2018. Projected change in characteristics of near surface temperature inversions for Southeast Australia. Clim. Dynam. 52 (3), 1487–1503.

Ji, F., Evans, J.P., Di Virgilio, G., Nishant, N., Di Luca, A., Herold, N., Beyer, K., 2020. Projected changes in vertical temperature profiles for Australasia. Clim. Dynam. 1–16.

Kalnay, E., Kanamitsu, M., Kistler, R., Collins, W., others, 1996. The NCEP/NCAR 40-year reanalysis project. Bull. Am. Meteorol. Soc. 77, 437–472.

Kjellström, E., Bärring, L., Nikulin, G., Nilsson, C., Persson, G., Strandberg, G., 2016. Production and use of regional climate model projections—a Swedish perspective on building climate services. Clim. Serv. 2 (3), 15–29. https://doi.org/10.1016/j.clise.r.2016.06.004.

Knutti, R., Sedláček, J., 2013. Robustness and uncertainties in the new CMIP5 climate model projections. Nat. Clim. Change 3, 369–373. https://doi.org/10.1038/nclimate1716.

Li, Y.B., Tam, C.Y., Huang, W.R., Cheung, K.K., Gao, Z., 2016. Evaluating the impacts of cumulus, land surface and ocean surface schemes on summertime rainfall simulations over East-to-southeast Asia and the western north Pacific by RegCM4. Clim. Dynam. 46 (7–8), 2487–2505.

Lee, M.H., Lu, M.Q., Im, E.S., Bae, D.H., 2019. Added value of dynamical downscaling for hydrological projections in the Chungju Basin, Korea. Int. J. Climatol. 39, 516–531.

Li, J.W., Sharma, A., Evans, J.P., Johnson, F., 2018. Addressing the mischaracterization of extreme rainfall in regional climate model simulations - a synoptic pattern based bias correction approach. J. Hydrol. 56, 901–912.

Liu, J., Pu, Z., 2019. Does soil moisture have an influence on near-surface temperature? J. Geophys. Res. Atmos. 124, 6444–6466.

Liu, D.L., Wang, B., Evans, J.P., Ji, F., Waters, C., Macadam, I., Beyer, K., 2019. Propagation of climate model biases to biophysical modelling can complicate assessments of climate change impact in agricultural systems. Int. J. Climatol. 39 (1), 424–444.

Macadam, I., Argüeso, D., Evans, J.P., Liu, D.L., Pitman, A.J., 2016. The effect of bias correction and climate model resolution on wheat simulations forced with a regional climate model ensemble. Int. J. Climatol. 36 (14), 4577–4591.

Moise, A.F., Wilson, L., Grose, M., Whetton, P., Watterson, I., Bhend, J., Bathols, J., Hanson, Erwin T., Bedin, T., Heady, C., Rafter, T., 2015. Evaluation of CMIP3 and CMIP5 models over the Australian L.region to inform confidence in projections. Austral. Meteorol. Oceanogr. J. 65, 19–53.

Ning, L., Riddle, E.E., Bradley, R.S., 2012. Projected changes in climate extremes over the northeastern United States. J. Clim. 3289–3310. https://doi.org/10.1175/JCLI-D-14-00150.1.

Nishant, N., Sherwood, S.C., 2021. How strongly are mean and extreme precipitation coupled? Geophys. Res. Lett. 48, e2020GL092075 https://doi.org/10.1029/2020GL092075.

Nishant, N., Evans, J.P., Di Virgilio, G., Downes, S.M., Ji, F., Cheung, K.K.W., Tam, E., Miller, J., Beyer, K., Riley, M.L., 2021. Introducing NARCliM1.5: evaluating the performance of regional climate projections for Southeast Australia for 1950–2100. Earth's Future 9, e2020EF001833. https://doi.org/10.1029/2020EF001833.

Nishant, N., Ji, F., Guo, Y., Herold, N., Green, D., Di Virgilio, G., Beyer, K., Riley, M.L., Perkins-Kirkpatrick, S., 2022. Future population exposure to Australian heatwaves. Environ. Res. Lett. 17 (6), 064030 https://doi.org/10.1088/1748-9326/ac6dfa.

Olson, R., Evans, J.P., Di Luca, A., Argueso, D., 2016. The NARCliM project: model agreement and significance of climate projections. Clim. Res. 69.

Ongoma, V., Chen, H., Gao, C., Nyongesa, A.M., Polong, F., 2018. Future changes in climate extremes over Equatorial East Africa based on CMIP5 multimodel ensemble. Nat. Hazards 90 (2), 901–920.

Pei, F., Zhou, Y., Xia, Y., 2021. Assessing the impacts of extreme precipitation change on vegetation activity. Agriculture 11 (6), 487.

Pepler, A.S., Di Luca, A., Ji, F., Alexander, L.V., Evans, J.P., Sherwood, S.C., 2016. Projected changes in east Australian midlatitude cyclones during the 21st century. Geophys. Res. Lett. 43 (1), 334–340.
Perkins-Kirkpatrick, S.E., Gibson, P.B., 2017. Changes in regional heatwave characteristics as a function of increasing global temperature. Sci. Rep. 7 (1), 1–12.
Perkins-Kirkpatrick, S.E., White, C.J., Alexander, L.V., Argueso, D., Boschat, G., Cowan, T., Evans, J.P., Ekstrom, M., 2016. Nat. hazards in Australia: Heatwaves, Clim. Change 139, 101–114.
Potter, N.J., Chiew, F.H., Charles, S.P., Fu, G., Zheng, H., Zhang, L., 2020. Bias in dynamically downscaled rainfall characteristics for hydroclimatic projections. Hydrol. Earth Syst. Sci. 24 (6), 2963–2979.
Prein, A.F., Rasmussen, R.M., Ikeda, K., Liu, C., Clark, M.P., Holland, G.J., 2017. The future intensification of hourly precipitation extremes. Nat. Clim. Change 7 (1), 48–52.
Qiu, L.Y., Im, E.S., 2021. Added value of high-resolution climate projections over South Korea on the scaling of precipitation with temperature. Environ. Res. Lett. 16, 124034.
Schulzweida, U., Kornblueh, L., Quast, R., 2006. CDO user's guide. Climate data operators, Version, 1, pp. 205–209, 6.
Seneviratne, S.I., Nicholls, N., Easterling, D., Goodess, C.M., Kanae, S., Kossin, J., Luo, Y., Marengo, J., McInnes, K., Rahimi, M., Reichstein, M., Sorteberg, A., Vera, C., Zhang, X., 2012. Changes in climate extremes and their impacts on the natural physical environment. In: Field, C.B., Barros, V., Stocker, T.F., Qin, D., Dokken, D.J., Ebi, K.L., Mastrandrea, M.D., Mach, K.J., Plattner, G.-K., Allen, S.K., Tignor, M., Midgley, P.M. (Eds.), Managing the Risks of Extreme Events and Disasters to Advance Climate Change Adaptation, pp. 109–230. A Special Report of Working Groups I and II of the Intergovernmental Panel on Climate Change (IPCC). Cambridge University Press, Cambridge, UK, and New York, NY, USA.
Skamarock, W.C., Klemp, J.B., 2008. A time-split nonhydrostatic atmospheric model for weather research and forecasting applications. J. Comput. Phys. 227 (7), 3465–3485.
Skelton, M., Porter, J.J., Dessai, S., Bresch, D.N., Knutti, R., 2017. The social and scientific values that shape national climate scenarios: a comparison of The Netherlands, Switzerland and the UK. Reg. Environ. Change 17, 2325–2338. https://doi.org/10.1007/s10113-017-1155-z.
Solman, S.A., Blázquez, J., 2019. Multiscale precipitation variability over South America: analysis of the added value of CORDEX RCM simulations. Clim. Dynam. 53 (3–4), 1547–1565.
Solomon, S., Manning, M., Marquis, M., Qin, D., 2007. Climate Change 2007-the Physical Science Basis: Working Group I Contribution to the Fourth Assessment Report of the IPCC (Vol. 4). Cambridge university press.
Tabari, H., 2020. Climate change impact on flood and extreme precipitation increases with water availability. Sci. Rep. 10 (1), 1–10.
Taylor, K.E., 2001. Summarizing multiple aspects of model performance in a single diagram. J. Geophy. Res. 106, 7183–7192.
Tebaldi, C., Arblaster, J.M., Knutti, R., 2011. Mapping model agreement on future climate projections. Geophys. Res. Lett. 38.
Torma, C., Giorgi, F., Coppola, E., 2015. Added value of regional climate modeling over areas characterized by complex terrain—precipitation over the Alps. J. Geophys. Res. Atmos. 120 (9), 3957–3972.
Vogel, E., Donat, M.G., Alexander, L.V., Meinshausen, M., Ray, D.K., Karoly, D., Meinshausen, N., Frieler, K., 2019. The effects of climate extremes on global agricultural yields. Environ. Res. Lett. 14, 054010.
Wang, X., Jiang, D., Lang, X., 2017. Future extreme climate changes linked to global warming intensity. Sci. Bull. 62 (24), 1673–1680.
Wang, B., Liu, D.L., Evans, J.P., Ji, F., Waters, C., Macadam, I., Beyer, K., 2019. Modelling and evaluating the impacts of climate change on three major crops in south-eastern Australia using regional climate model simulations. Theor. Appl. Climatol. 138 (1–2), 509–526.
Zander, K.K., Botzen, W.J., Oppermann, E., Kjellstrom, T., Garnett, S.T., 2015. Heat stress causes substantial labour productivity loss in Australia. Nat. Clim. Change 5 (7), 647–651.
Zhou, L., Dai, Q., Han, D.W., Chen, N.S., Zhao, B.R., 2019. Assessment of simulated soil moisture from WRF Noah, noah-MP, and CLM land surface schemes for landslide hazard application. Hydrol. Earth Syst. Sci. https://doi.org/10.5194/hess-2019-9.
Zhu, Q., Yang, X., Ji, F., Liu, D.L., Yu, Q., 2019. Extreme rainfall, rainfall erosivity, andhillslope erosion in Australian Alpine region and theirfuture changes. Int. J. Climatol. 2019, 1–15. https://doi.org/10.1002/joc.6266.
Zivin, J.G., Shrader, J., 2016. Temperature extremes, health, and human capital. Future Child. 26 (1), 31–50.